BIOMOLECULES & THERAPEUTICS

Original Article
Biomol Ther 29(5), 519-526 (2021)

Cyclooxygenase-2 Inhibitor Parecoxib Was Disclosed as a PPAR-γ Agonist by *In Silico* and *In Vitro* Assay

Bin Xiao[1,†], Dan-dan Li[2,†], Ying Wang[2], Eun La Kim[2], Na Zhao[1], Shang-Wu Jin[3], Dong-Hao Bai[3], Li-Dong Sun[3,*] and Jee H. Jung[2,*]

[1]Laboratory of Clinical Pharmacy, Ordos Central Hospital, Ordos School of Clinical Medicine, Inner Mongolia Medical University, Ordos 017000, China
[2]College of Pharmacy, Pusan National University, Busan 46241, Republic of Korea
[3]The Fourth People's Hospital of Ordos, Ordos 017000, China

Abstract

In a search for effective PPAR-γ agonists, 110 clinical drugs were screened via molecular docking, and 9 drugs, including parecoxib, were selected for subsequent biological evaluation. Molecular docking of parecoxib to the ligand-binding domain of PPAR-γ showed high binding affinity and relevant binding conformation compared with the PPAR-γ ligand/antidiabetic drug rosiglitazone. Per the docking result, parecoxib showed the best PPAR-γ transactivation in Ac2F rat liver cells. Further docking simulation and a luciferase assay suggested parecoxib would be a selective (and partial) PPAR-γ agonist. PPAR-γ activation by parecoxib induced adipocyte differentiation in 3T3-L1 murine preadipocytes. Parecoxib promoted adipogenesis in a dose-dependent manner and enhanced the expression of adipogenesis transcription factors PPAR-γ, C/EBPα, and C/EBPβ. These data indicated that parecoxib might be utilized as a partial PPAR-γ agonist for drug repositioning study.

Key Words: Parecoxib, *In silico* screening, PPAR-γ agonist, Adipogenesis

INTRODUCTION

Peroxisome proliferator-activated receptors (PPARs) are members of the nuclear receptor superfamily of ligand-activated transcription factors and comprised three subtypes: PPAR-α, β/δ, and γ (Mangelsdorf *et al*., 1995; Berger and Moller, 2002; Evans *et al*., 2004). In particular, PPAR-γ is expressed in adipose tissue, colon, and macrophages and plays essential roles in the regulation of lipid metabolism, adipogenesis, glucose homeostasis, and insulin sensitization (Willson *et al*., 2001; Semple *et al*., 2006; Higgins and Mantzoros, 2008); hence, PPAR-γ is the target for drug discovery efforts for diseases such as type 2 diabetes mellitus (T2DM) (Higgins and Mantzoros, 2008). Although PPAR-γ agonists such as thiazolidinediones (TZDs; e.g., rosiglitazone and troglitazone, Fig. 1A) have been used to treat T2DM for many years in clinical practice and have been shown to lower blood glucose levels and improve insulin sensitivity (Elte and Blickle, 2007), the adverse effects including increased risk of heart attack, weight gain, edema, and fluid retention remain to be challenged. Therefore, new PPAR-γ ligands with less adverse effects are still in demand for T2DM treatment (Motoshima *et al*., 2011). In addition to TZDs (Petersen *et al*., 2011), a series of synthetic L-tyrosine analogs (e.g., farglitazar and muraglitazar, Fig. 1A) have been developed as PPAR-γ agonists and subjected to phase II clinical trials (Cobb *et al*., 1998; Collins *et al*., 1998; Henke *et al*., 1998). Linoleic acid, α-linolenic acid, and prostanoid 15-deoxy-$^{\Delta 12,14}$-PGJ$_2$ (15d-PGJ$_2$) are known as putative endogenous ligands for PPAR-γ with relatively low affinities (Fig. 1B) (Forman *et al*., 1995; Krey *et al*. 1997; Berger and Moller, 2002). All known PPAR-γ ligands comprise three distinct substructures —a polar head, linker, and hydrophobic tail (Fig. 2).

In recent years, computational methods have become an integral approach to screen and design novel bioactive compounds. However, a drug repositioning study with a combination of molecular docking and biological evaluation of known pharmacophores will be a promising method to develop new

Open Access **https://doi.org/10.4062/biomolther.2021.008**

Received Jan 11, 2021 **Revised** Mar 26, 2021 **Accepted** Mar 31, 2021
Published Online Apr 22, 2021

***Corresponding Authors**
E-mail: 935194526@qq.com (Sun LD), jhjung@pusan.ac.kr (Jung JH)
Tel: +86-477-8185276 (Sun LD), +851-510-2803 (Jung JH)
Fax: +86-477-8185276 (Sun LD), +851-513-6754 (Jung JH)
[†]The first two authors contributed equally to this work.

bioactive leads (Hu *et al*., 2017). In this study, we screened 110 clinically used drugs for binding affinity to the PPAR-γ ligand-binding domain (LBD) via molecular docking, and 9 drugs, including parecoxib, were selected for subsequent biological analyses. Among these, parecoxib showed the best PPAR-γ binding affinity (Table 1).

The cyclooxygenase-2 (COX-2) inhibitor parecoxib is clinically used to relieve pain, inflammation, central sensitization, and postoperative cognitive dysfunction (Bian *et al*., 2018; Huang *et al*., 2019; Wang *et al*., 2019). However, there was no report on the therapeutic potential of parecoxib through activation of PPAR-γ. Parecoxib is metabolized to the active metabolite valdecoxib in a biological system. The structure of parecoxib may be depicted as a collection of three distinct partial structures, i.e., a polar head, linker, and hydrophobic tail, similar to other typical PPAR-γ agonists (Fig. 2). Therefore, we explored the pharmacological potential of parecoxib as a PPAR-γ agonist with regard to drug reposition.

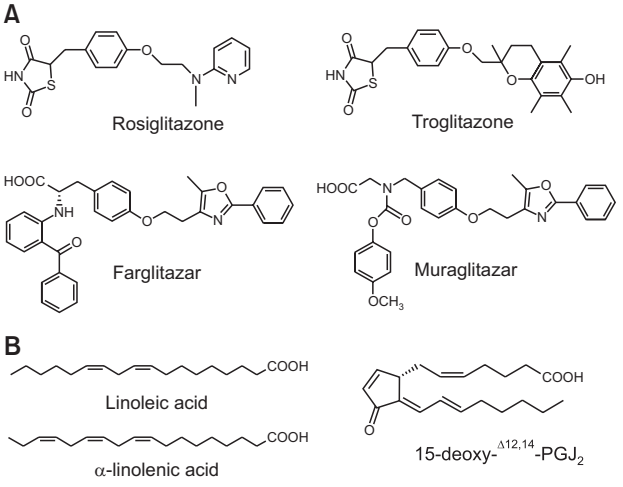

Fig. 1. Structures of natural or synthetic PPAR-γ agonists. (A) Representative synthetic PPAR-γ agonists; (B) putative endogenous PPAR-γ agonists.

MATERIALS AND METHODS

Materials

Rosiglitazone, cefazolin, omeprazole, furosemide, esomeprazole, parecoxib, ondansetron, and linezolid were purchased from Sigma-Aldrich (St. Louis, MO, USA) with more than 98% purity. All compounds were dissolved in dimethylsulfoxide (Sigma-Aldrich) at 20 mM concentration. 3-Isobutyl-1-methylxanthine (IBMX), dexamethasone, and insulin were obtained from Sigma-Aldrich and dissolved in 0.5 M KOH, 100% ethanol, and 0.02 M HCl, respectively.

Computational methods

For molecular docking, protein coordinates were downloaded from the Protein Data Bank (accession code: 2PRG) (Berman *et al*., 2000). Chain A was prepared for docking using the molecular modeling software package Chimera 1.5.3 (National Institutes of Health, Bethesda, MD, USA) (Pettersen *et al*., 2004). Polar hydrogen and setting grid box parameters were added using MGLTools 1.5.4 (The Scripps Research Institute, La Jolla, CA, USA) (Sanner, 1999; Morris *et al*., 2009). Docking calculations were performed using AutoDock Vina 1.1.2

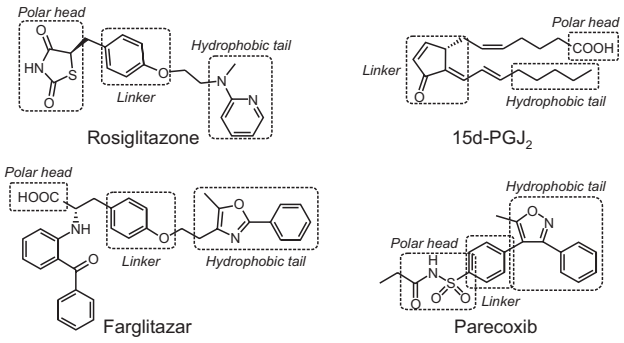

Fig. 2. Graphical illustration of the key pharmacophore concept of rosiglitazone, 15d-PGJ_2, farglitazar, and parecoxib. These chemical entities are considered as a combination of a polar head, linker, and hydrophobic (compared to the polar head) tail.

Table 1. PPAR-γ docking simulation results of selected drugs

Drug	Bioactivity[a]	Drug target[b]	Binding affinity (kcal/mol)	H-bond
Rosiglitazone	Antidiabetic	PPAR-γ	–9.0	Tyr^{473}/Arg^{288}/His^{323}/Ser^{289}/Gln^{286}
Cefazolin	Antibacterial	PBPs	–7.8	Tyr^{473}/His^{323}/Arg^{288}/Glu^{343}
Papaverine	Smooth muscle relaxant	phosphodiesterase	–8.0	Ser^{342}/Arg^{288}
Omeprazole	PPI	H^+/K^+-ATPase	–8.0	Ser^{342}/Tyr^{473}
Furosemide	Diuretic	NKCC2	–7.4	Glu^{343}/Gly^{284}/Arg^{288}/Leu^{340}
Esomeprazole	PPI	H^+/K^+-ATPase	–8.0	Ser^{342}/Tyr^{327}
Parecoxib	Analgesic	COX-2	–9.4	Tyr^{327}/Ser^{289}/His^{323}
Ondansetron	Antiemetic	5-HT3	–7.9	Ser^{342}
Valdecoxib	Analgesic	COX-2	–8.8	Tyr^{327}/Ser^{289}
Linezolid	Antibacterial	50S	–8.2	Glu^{343}/Tyr^{327}/Arg^{288}

[a]PPIs, proton pump inhibitors; [b]PBPs, penicillin-binding proteins; NKCC2, Na-K-Cl cotransporter 2; 50S, the larger subunit of the 70S ribosomes of prokaryotes; 5-HT3, 5-hydroxytryptamine receptor 3; COX-2, cyclooxygenase 2; PPAR-γ, peroxisome proliferator-activated receptor γ. Binding affinity is shown as kcal/mol. Omeprazole is a racemate, and esomeprazole is an (*S*)-isomer. However, tetrahedral configuration of the sulfoxide could not be generated by Chemdraw software, so the planar configuration, instead of a tetrahedral configuration, was employed for docking.

software (The Scripps Research Institute) (Trott and Olson, 2010). The default settings and the Vina scoring function were applied. For ligand preparation, Chem3D Ultra 8.0 software (CambridgeSoft Corporation, Cambridge, MA, USA) was used to convert the 2D structures of candidates into 3D structural data. The analysis and visual investigation of ligand-protein interactions of docking poses were performed using PyMol v1.5 (Schrodinger LLC, New York, NY, USA).

Cell culture

Rat liver cells (AC2F), human hepatoma cells (HepG2), and preadipocytes cells (3T3-L1) were obtained from American Type Culture Collection (ATCC, VA, USA) and cultured in Dulbecco's Modified Eagle's medium (Hyclone, Logan, UT, USA) supplemented with 10% fetal bovine serum (FBS, Gibco-BRL, NY, USA) and 1% penicillin/streptomycin at 37°C containing 5% CO_2.

Cell viability

AC2F and 3T3-L1 cells (1×10^4 cells/well) were seeded into a 96-well plate. After 12 h, the cells were treated with parecoxib at different concentrations (5, 10, 20, 40, and 80 μM) for 12 h or 48 h. After treatment, 0.5 mg/mL of 3-(4, 5-dimethylthiazol-2-yl)-2,5-diphenyltetrazolium bromide (MTT) was added into every well and incubated for another 4 h in the dark. After discarding the medium containing MTT, 150 μL DMSO was added to every well to dissolve the formazan crystals, and the optical density value was measured using a microplate reader (Elx 800, Bio-Tek, Winooski, VT, USA) at 490 nm.

PPAR-γ (-α/-β/δ) transactivation assay

AC2F cells (5×10^4 cells/well) were seeded into a 48-well plate and cultured overnight. As the cells achieved 90% confluence, they were transferred into effector plasmids, 1 μg TK-PPRE×3-luciferase reporter plasmid, 0.1 μg PcDNA, and 0.1 μg pFlag-PPAR-γ1 using Lipofectamine™ 2000 (Invitrogen, Carlsbad, CA, USA), according to a previously described protocol (Eom *et al*., 2016). After 4 h, the conditioned culture media were replaced with a complete medium, and the cells were incubated for 20 h. Subsequently, the complete medium was discarded, and the cells were treated with rosiglitazone, PPAR-α agonist (WY-14643), PPAR-β/δ agonist (GW501516), and parecoxib in serum-free medium for another 6 h. After treatment, the cells were lysed using ONE-Glo™ Luciferase Assay System regent (Promega Co., WI, USA), and PPAR-γ activities were analyzed using GloMax®-Multi Microplate Multimode Reader (Promega Co.). PPAR-α and PPAR-β/δ transactivation was measured in the same manner using pFlag-PPAR-α/PPAR-β/δ.

Adipocyte differentiation assay

Preadipocytes (3T3-L1, 5×10^4 cells/well) were seeded into a 48-well plate and the cells were incubated until 100% confluent. Subsequently, fresh media were replaced, and the cells were cultured for another 2 days (day 0). Furthermore, the media were changed to MDI induction media, containing 10% FBS, 0.5 mM IBMX, 1 μM dexamethasone, and 1 μg/mL insulin, and treated in the presence of rosiglitazone (1 μM) or parecoxib (15, 30, and 60 μM) (day 2). After 2 days, the media were changed to insulin media, containing 10% FBS and 1 μg/mL insulin, and treated with rosiglitazone (1 μM) or parecoxib (15, 30, and 60 μM) (day 4). After 2 days, the media were replaced with complete media and treated with the drugs for another 4 days (day 8), and the mature adipocytes were obtained.

On day 8, the media were removed, and cells were washed with phosphate buffered saline. The cells were then fixed with 70% ethanol for 30 min and stained with Oil Red O for 1 h. After washing with dH_2O, an Optinity (Gyeonggi, Korea) microscope was used to capture images. To elute the Oil Red O staining, 100% isopropanol was used. The OD value was determined using iMark Microplate Absorbance Reader (Bio-Rad Laboratories, Hercules, CA, USA) at 544 nm.

Western blot assay

The Ac2F cells and adipocytes (after differentiation) were seeded in 60 mm dishes overnight. The dishes were treated with parecoxib (15, 30, and 60 μM) and rosiglitazone (10 μM) and incubated for 48 h. After treatment, the total protein was extracted using radioimmunoprecipitation assay buffer containing a protease inhibitor mixture of 1% PMSF, 1% aprotinin, and 1% pepstatin. Nuclear protein was extracted using NE-PER® nuclear and cytoplasmic extraction reagents (Thermo Scientific, Rockford, IL, USA) containing 1% PMSF, 1% aprotinin, and 1% pepstatin. BCA kit was used to confirm the protein concentration. The total and nuclear proteins were separated through sodium dodecyl sulfate-polyacrylamide gel electrophoresis (SDS-PAGE) and then transferred onto polyvinylidene fluoride membranes. The membranes were blocked by 5% milk at 25°C for 2 h and then incubated by PPAR-γ (Cell Signaling Technology, USA), C/EBPα (Cell Signaling Technology), C/EBPβ (Cell Signaling Technology) antibodies at 4°C overnight. On the second day, the membranes were washed using Tris buffered saline with Tween-20 and incubated with Anti-rabbit horseradish-linked IgG for 1 h. Enhanced chemiluminescent reagent and the ChemiDoc™ Touch Imaging System (Bio-Rad Laboratories) were used to analyze the protein band.

Immunofluorescence staining

The Ac2F cells and adipocytes (after differentiation) were seeded into the confocal dishes overnight. The cells were treated with parecoxib (15, 30, and 60 μM) and rosiglitazone (10 μM) for 48 h. Then, the cells were fixed with formalin for 10 min. The permeabilization of cells was achieved by incubating the cells with 0.3% Triton X-100 for 15 min. Next, the cells were blocked using 10% FBS and incubated with a PPAR-γ antibody at 4°C overnight. The cells were incubated with anti-mouse Alexa 488 secondary antibodies (Cell Signaling Technology) for 30 min, and then PI (10 μg/mL) and RNase (10 μg/mL) reagents were added to the cells and incubated for 40 min. Finally, FluoView FV10i confocal microscope (Olympus, Tokyo, Japan) was used to analyze the stained cells.

Statistics

Data were analyzed using GraphPad Prism 5 (GraphPad Software, San Diego, CA, USA). The significance between groups was analyzed using one-way analysis of variance and tukey's range test. All results are expressed as means ± standard error of the mean, and $p<0.05$ was considered significant.

RESULTS

Docking simulations of clinical drugs to PPAR-γ

One-by-one molecular docking was performed to gain insight into the interaction between ligand and PPAR-γ *in silico* screening.

For *in silico* screening, compounds of molecular weight less than 500 amu (Lipinski *et al*., 1997) were selected from 110 clinical drugs used in Ordos Central Hospital. Nine clinical drugs (cefazolin, papaverine, omeprazole, furosemide, esomeprazole, parecoxib, ondansetron, valdecoxib, and linezolid) with substantial binding affinities (ranging from –7.4 kcal/mol to –9.4 kcal/mol) and valid binding conformations (bound to the PPAR-γ LBD and formed H-bonds with key amino acid residues) were selected (Table 1). In particular, parecoxib showed a strong binding affinity (–9.4 kcal/mol) when compared with other clinical drugs and the standard PPAR-γ agonist rosiglitazone (–9.0 kcal/mol).

Rosiglitazone formed hydrogen bonds with key amino acids Ser^{289}(H3), Arg^{288}(H3), Gln^{286}(H3), His^{323}(H11), and Tyr^{473}(H12) residues on helices H3, H11, and H12 in the PPAR-γ LBD (Fig. 3A). It is known that rosiglitazone stabilizes the dynamic H12 region through the aforementioned interactions and activates PPAR-γ. Parecoxib showed hydrogen bonding with Ser^{289} (H3), Tyr^{327}(H5), His^{323}(H11) residues on helices H3, H5, and H11 (Fig. 3B). The simulation data indicated that parecoxib skeleton might be suitable for PPAR-γ LBD (Fig. 3B); the sulfonyl propanamide moiety may serve as a head group forming H-bonds with key amino acids Ser289(H3), Tyr327(H5), and His323(H11) in the PPAR-γ LBD, whereas the phenyl group serves as a linker, and the 5-methyl-3-phenylisoxazol-4-yl moiety serves as a hydrophobic tail positioned in the hydrophobic binding pocket. However, the binding conformation of parecoxib lacked the key hydrogen bonding with Tyr^{473}(H12), which was observed for rosiglitazone. Instead, parecoxib seems to be positioned between the helix 3 (H3) and the -sheet to stabilize this part, which is a typical binding profile of partial agonists, such as amorfrutin (Wang *et al*., 2014). Partial PPAR- agonists are proposed to be useful as antidiabetic agents because it would be free of side effects of full agonists (Kroker and Bruning, 2015).

Parecoxib is metabolized to valdecoxib (amide moiety being hydrolyzed) after absorption into the human body, and finally, valdecoxib itself manifests COX-2 inhibition. Therefore, the pharmacologically active valdecoxib was also assessed for *in silico* PPAR-γ binding (Fig. 3C). Valdecoxib showed a lower binding affinity (–8.8 kcal/mol) than parecoxib (–9.4 kcal/mol). Parecoxib showed hydrogen bonding with Ser^{289}, Tyr^{327}, and His^{323} residues on helices H3, H5, and H11 (Fig. 3B). Furthermore, valdecoxib showed hydrogen bonding with only Tyr^{327} and Ser^{289}. The interaction between ligand and Tyr^{473} is suggested to be essential for the activation of PPAR-γ by a full agonist such as rosiglitazone.

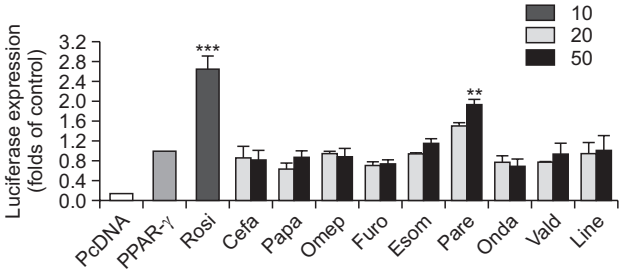

Fig. 4. PPAR-γ activation of nine clinical drugs and rosiglitazone. Ac2F cells were transfected with PcDNA, PPRE, and/or pFlag-PPAR-γ1, and then treated with nine clinical drugs (20 μM and 50 μM) and rosiglitazone (10 μM parecoxib and rosiglitazone in Ac2F cells) for 6 h. PPAR-γ activation was measured using luciferase expression assay. Rosi: rosiglitazone, cefa: cefazolin, papa: papaverine, omep: omeprazole, furo: furosemide, esom: esomeprazole, pare: parecoxib, onda: ondansetron, vald: valdecoxib, line: linezolid. Ac2F cells were transfected with PcDNA as the blank group. Control group cells were transfected with PPRE and pFlag-PPAR-1. Triplicate wells were used in every sample group and the experiments were repeated for three times. **p<0.01, ***p<0.001 vs. PPAR-γ.

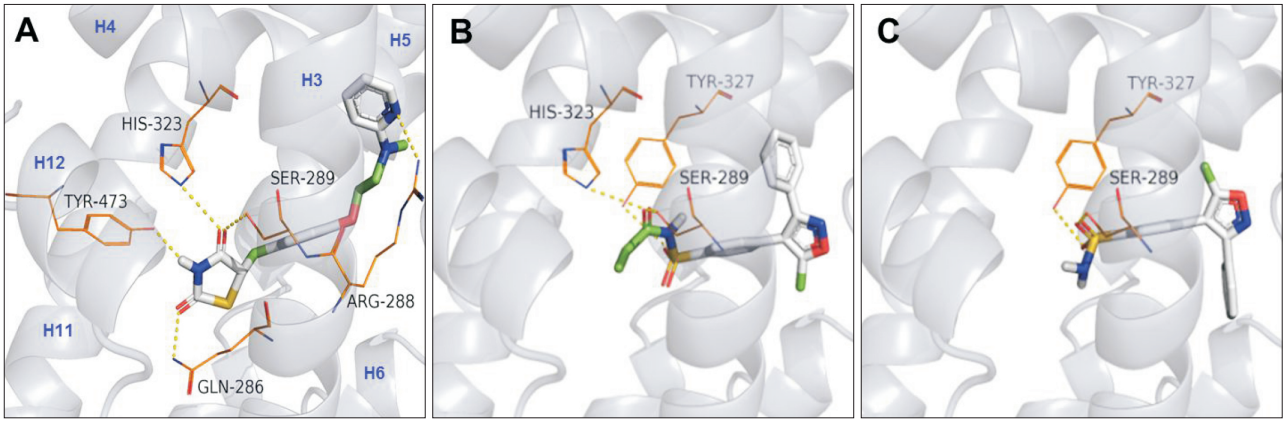

Fig. 3. Docking structures of ligand/PPARγ binding. (A) Zoomed view of the hydrogen bonding interactions (yellow dotted lines) between the rosiglitazone and surrounding amino acids Ser^{289}(H3), Arg^{288}(H3), Gln^{286}(H3), His^{323}(H11), and Tyr^{473}(H12) on helices H3, H11, and H12. Helices of PPAR-γ are labeled in blue. (B) Zoomed view of the hydrogen bonding interactions between parecoxib and surrounding amino acids Ser^{289}(H3), Tyr^{327}(H5), and His^{323}(H11) on helices H3, H5, and H11. (C) Zoomed view of the hydrogen bonding interactions between valdecoxib and surrounding amino acids Ser^{289}(H3) and Tyr^{327}(H5).

PPAR-γ transactivation by parecoxib

The PPAR-γ transactivation activity of nine clinical drugs was evaluated using Ac2F rat liver cells. Consistent with molecular docking, luciferase expression assay demonstrated that parecoxib has the best effect on PPAR-γ activation, though it was not as potent as rosiglitazone (Fig. 4). The effect of parecoxib on PPAR-γ transactivation was further examined at various concentrations. Prior to the PPAR-γ transactivation assay using Ac2F cells, the cytotoxicity of parecoxib to Ac2F cells was measured using MTT assay (Fig. 5A). The concentrations for the PPAR-γ transactivation assay were chosen from five non-cytotoxic concentrations. Parecoxib activated PPAR-γ in a dose-dependent manner (Fig. 5D). The effect of parecoxib on the PPAR isoforms PPAR-α and PPAR-β/δ was also investigated in comparison to PPAR-α agonist (WY-14643) and PPAR-β/δ agonist (GW501516), respectively (Fig. 5B, 5C). Parecoxib showed lesser activity to PPAR-α than rosiglitazone, and was non-active to PPAR-β/δ.

Once the PPAR-γ ligand binds to the receptor, the activated PPAR-γ will transfer to the cell nucleus and bind to PPRE to regulate subsequent gene expression (Su *et al*., 2017). Therefore, the level of endonuclear PPAR-γ was detected using western blot and immunofluorescence staining assay. As shown in Fig. 6A, parecoxib significantly increased the endonuclear PPAR-γ concentration in Ac2F cells, similar to rosiglitazone. A significant level of PPAR-γ protein was detected as green fluorescence in the nuclei of parecoxib (60 μM)-treated and rosiglitazone (10 μM)-treated groups (Fig. 6B). This indicated that parecoxib activated PPAR-γ and promoted endonuclear PPAR-γ translocation. Thus, parecoxib was defined as a potential PPAR-γ activator.

Adipocyte differentiation in 3T3-L1 cells

In this study, the adipogenic activity of parecoxib was examined using murine preadipocytes (3T3-L1). 3T3-L1 cells were treated with IBMX, dexamethasone, insulin plus rosiglitazone, or different parecoxib concentrations for 8 days. Lipid droplets accumulated by adipogenesis can be visualized through red color by Oil Red O staining. The Oil Red O staining showed that parecoxib stimulated adipogenesis in a dose-dependent

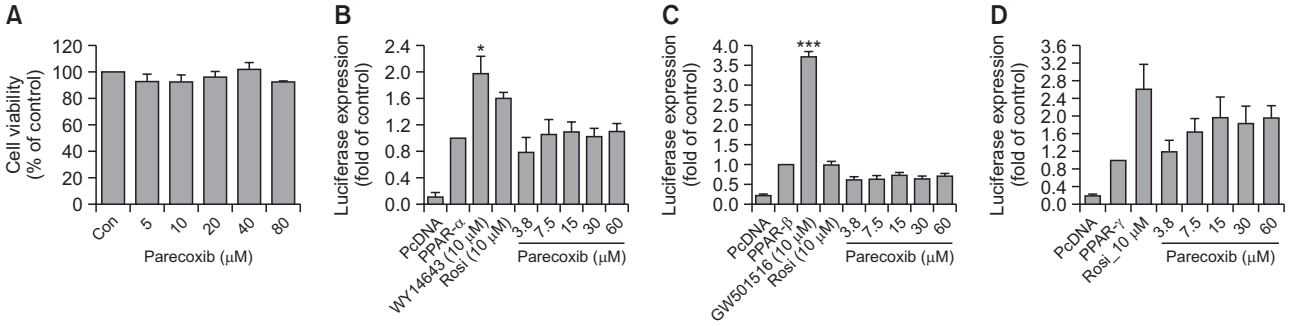

Fig. 5. Effects of parecoxib on transactivation of PPAR-α, β/δ, and γ. (A) Cytotoxicity of parecoxib to Ac2F cells. Ac2F cells were treated with parecoxib for 12 h, and cell viability was measured using MTT assay. (B) Transactivation of PPAR-α by parecoxib. WY-14643 was employed as a standard PPAR-α agonist. (C) Transactivation of PPAR-β/δ by parecoxib. GW501516 was employed as a standard PPAR-β/δ agonist. (D) Concentration-dependent PPAR-γ transactivation by parecoxib. PcDNA, PPRE, PPAR-α, PPAR-β/δ, and PPAR-γ plasmids were transfected into Ac2F cells, and the cells were treated by parecoxib, WY-14643, GW501516, or rosiglitazone for 6 h. Ac2F cells were transfected with PcDNA as the blank group. Control group cells were transfected with PPRE and PPAR-α, β/δ, or γ1. Triplicate wells were used in every sample group and the experiments were repeated for three times. **p*<0.05, ****p*<0.001 vs. PPAR-α or β/δ.

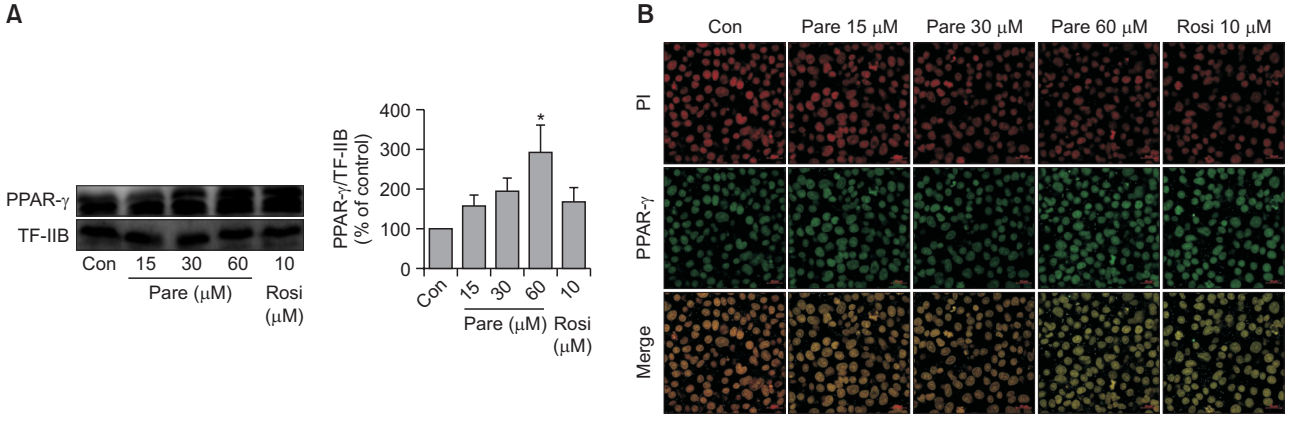

Fig. 6. Detection of endonuclear protein levels of PPAR-γ. (A) Endonuclear protein level of PPAR-γ in Ac2F cells was detected by western blot assay after treating with parecoxib (15, 30, and 60 μM) and rosiglitazone (10 μM). Transcription Factor II B was employed as a control. (B) Immunofluorescence staining of endonuclear PPAR-γ in Ac2F cells after treating with parecoxib and rosiglitazone. The experiments were repeated for three times. **p*<0.05 vs. control.

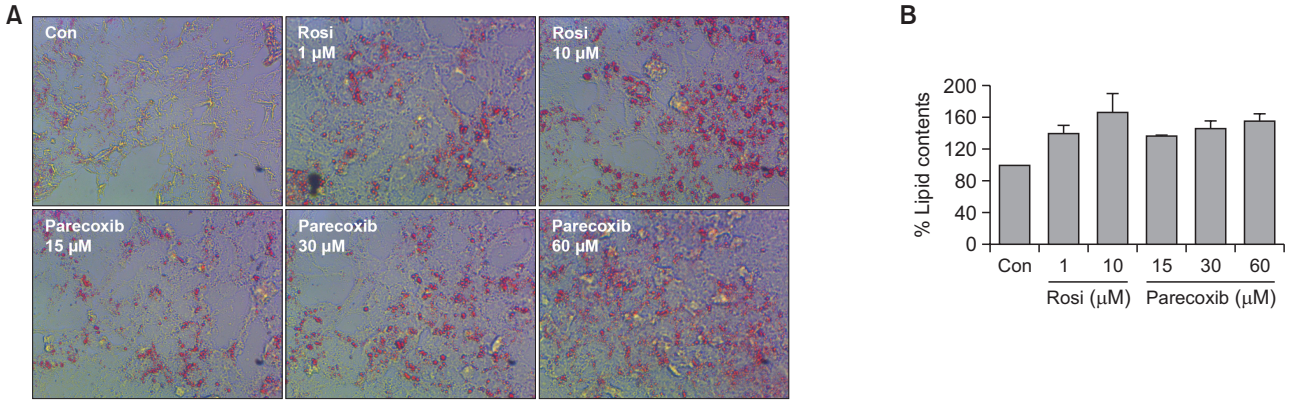

Fig. 7. Effect of parecoxib on adipocyte differentiation in 3T3-L1 cells. (A) Morphological assessment of adipocyte differentiation by microscopy. The 3T3-L1 cells were treated with 10% FBS, 0.5 mM IBMX, 1 μM dexamethasone, 1 μg/ml insulin, and rosiglitazone (1 μM, 10 μM) or various concentrations of parecoxib (15, 30, and 60 μM) for 8 d, and then stained with Oil Red O. Mature adipocytes are shown as red droplets. (B) Assessment of lipid accumulation in the adipocytes. Lipid content was measured in 100% isopropanol as OD value using iMark Microplate Absorbance Reader. Triplicate wells were used in every sample group and the experiments were repeated for three times. Pare, parecoxib; Rosi, rosiglitazone.

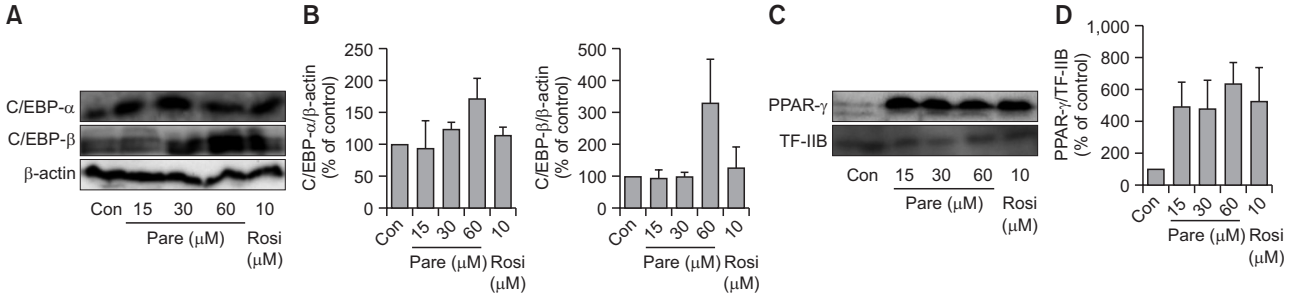

Fig. 8. Protein levels of adipogenesis transcription factors PPAR-γ, C/EBPα, and C/EBPβ in 3T3-L1 cells were determined using western blot assay after treating with parecoxib or rosiglitazone (A) The bands of C/EBPα and C/EBPβ. β-actin was employed as controls. (B) The quantitative analysis of C/EBPα and C/EBPβ. (C) The band of endonuclear PPAR-γ. TF-IIB was employed as a control for nuclear protein. (D) The quantitative analysis of endonuclear PPAR-γ. The experiments were repeated for three times. Pare, parecoxib; Rosi, rosiglitazone.

manner (Fig. 7A). The preadipocytes were well-differentiated into mature adipocytes following rosiglitazone or parecoxib treatment (shown as red lipid in Fig. 7A), and this microscopic observation was well correlated with the concentration-dependent increase in total lipid accumulation in adipocytes (Fig. 7B).

Subsequently, the expression of C/EBPα and C/EBPβ and the protein level of PPAR-γ in the nucleus were compared using western blot and immunofluorescence staining assay. As shown in Fig. 8A and 8B, parecoxib increased the expression level of C/EBPα and C/EBPβ in 3T3-L1 cells. Additionally, the endonuclear PPAR-γ protein level was increased when treated with parecoxib and rosiglitazone (Fig. 8C, 8D). This result demonstrated that parecoxib might promote endonuclear translocation of PPAR-γ. Consistent with the western blot, immunofluorescence staining assay also showed that parecoxib enhances endonuclear PPAR-γ protein level in 3T3-L1 cells (Fig. 9). Thus, parecoxib worked as a PPAR-γ agonist and promoted endonuclear PPAR-γ translocation in Ac2F cells and 3T3-L1 cells.

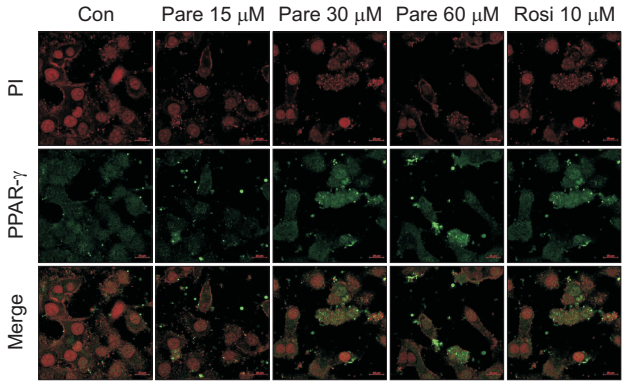

Fig. 9. Immunofluorescence staining of endonuclear PPAR-γ in 3T3-L1 cells. The experiments were repeated for three times. Pare, parecoxib; Rosi, rosiglitazone.

DISCUSSION

In this preliminary study on drug repositioning, a COX-2 inhibitor parecoxib was selected as a tentative PPAR-γ agonist via *in silico* analysis and *in vitro* evaluation of clinically used drugs. In docking simulations, parecoxib showed higher binding affinity than rosiglitazone, but its hydrogen bonding network was distinct from that of rosiglitazone. As for rosiglitazone, the hydrogen bonding with Tyr^{473} was suggested to be essential to induce H12 into active conformation and thereby activate PPAR-γ (Waku *et al*., 2009). However, parecoxib did not show direct hydrogen bonding with Tyr^{473} on the helix H12. Instead, it formed an alternative hydrogen bond with Tyr^{327} on the helix H5 and was positioned between H3 and β-sheet, stabilizing this region similar to the typical partial agonist amorfrutin.

Human apo-PPAR-γ LBD has a sizable binding pocket, and rosiglitazone occupies roughly 40% of the ligand-binding site in a U-shaped conformation (Nolte *et al*., 1998). Full agonist rosiglitazone forms hydrogen bonds with three key amino acid residues (His^{323}, His^{449}, and Tyr^{473}) to stabilize the AF-2 surface (Liu *et al*., 2015). The lack of these key interactions of parecoxib and valdecoxib may explain why they showed lower PPAR-γ transcriptional activity than rosiglitazone and indicate they might be PPAR-γ partial agonists. Partial agonists have lower efficacy than full agonists and occupy a partial cavity of the binding pocket and interact with partial amino acid residues. In addition, the *in vitro* assay demonstrated that parecoxib was a more potent PPAR-γ agonist than valdecoxib (the *in vivo* active form of parecoxib). Therefore, degradation-resistant parecoxib analog may be devised by modifying the hydrolysis-susceptible amide moiety of parecoxib. For example, branched alkyl chain or cyclic alkyl group may be introduced in place of the ethyl chain, to increase steric hindrance against enzymatic hydrolysis.

Cyclooxygenase-2 (COX-2) is up-regulated in diabetes mellitus, and selective inhibition of COX-2 could enhance the insulin secretion (Bagi *et al*., 2006; Fujita *et al*., 2007). Parecoxib, as a selective COX-2 inhibitor and PPAR-γ agonist, would serve as a lead for potential antidiabetic drug. Adipose tissues play a vital role in metabolic regulation and excess lipid storage (Camp *et al*., 2002). However, in type 2 diabetes, the ability of subcutaneous adipose tissue to recruit and differentiate precursor cells into adipocytes is reduced (Smith and Kahn, 2016). It is well-known that the PPAR-γ gene, which is abundant in adipose tissue, regulates adipogenesis and lipid metabolism (Chao *et al*., 2000; Wang *et al*., 2017). PPAR-γ stimulates the production of small insulin-sensitive adipocytes. Adipose tissue produces several cytokines that regulate energy homeostasis, lipid, and glucose metabolism. In addition to its importance in adipogenesis, PPAR-γ plays an essential role in regulating lipid metabolism in mature adipocytes by increasing fatty acid trapping (Leonardini *et al*., 2009). PPAR-γ agonistic drugs TZDs, such as rosiglitazone and troglitazone, show antidiabetic effects through targeting adipose tissue (Chao *et al*., 2000). The anti-inflammatory drug parecoxib showed PPAR-γ transactivation in a concentration-dependent mode in Ac2F rat liver cells. As a PPAR-γ agonist, parecoxib was exploited as a potential antidiabetic agent through *in vitro* evaluations, similar to rosiglitazone.

Adipocyte differentiation is a complex process that is regulated by a set of transcription factors such as PPAR-γ and CCAAT-enhancer-binding protein α/β (C/EBPα/β) (Jiang *et al*., 2019). PPAR-γ is a master regulator to induce adipogenesis. The protein C/EBPα belongs to a family of basic region/leucine zipper (bZip) transcription factors (Khanna-Gupta *et al*., 2012) which participate in adipogenesis along with PPAR-γ. Although the protein C/EBPβ is expressed in the early stage of adipocyte differentiation to activate the expression of PPAR-γ and C/EBPα, C/EBPβ together with PPAR-γ and C/EBPα then induce lipid accumulation or glucose uptake (Younce *et al*., 2009; Jiang *et al*., 2019). In this study, we found that parecoxib promoted differentiation of adipocytes in a concentration-dependent manner, stimulated the expression of adipogenesis transcription factors CEBPα and C/EBPβ, and promoted translocation of PPAR-γ into the nucleus in Ac2F and 3T3-L1 cells. Though the potency of parecoxib did not reach that of rosiglitazone, possibly because of its partially agonistic nature, a substantial activity was obtained at higher concentrations. According to our preliminary study, parecoxib may be eligible for drug repositioning study and further pharmacological study as a PPAR-γ agonist.

CONFLICT OF INTEREST

The authors declare that they have no competing interests.

ACKNOWLEDGMENTS

This research was supported by a 2-year grant from Pusan National University. We thank Hye Lim Byun and Sunwoo Yu for their sincere assistance in molecular docking calculations.

REFERENCES

Bagi, Z., Erdei, N., Papp, Z., Edes, I. and Koller, A. (2006) Up-regulation of vascular cyclooxygenase-2 in diabetes mellitus. *Pharmacol. Rep.* **58**, 52-56.

Berger, J. and Moller, D. E. (2002) The mechanisms of action of PPARs. *Annu. Rev. Med.* **53**, 409-435.

Berman, H. M., Westbrook, J., Feng, Z., Gilliland, G., Bhat, T. N., Weissig, H., Shindyalov, I. N. and Bourne, P. E. (2000) The protein data bank. *Nucleic Acids Res.* **28**, 235-242.

Bian, Y. Y., Wang, L. C., Qian, W. W., Lin, J., Jin, J., Peng, H. M. and Weng, X. S. (2018) Role of parecoxib sodium in the multimodal analgesia after total knee arthroplasty: a randomized double-blinded controlled trial. *Orthop. Surg.* **10**, 321-327.

Camp, H. S., Ren, D. and Leff, T. (2002) Adipogenesis and fat-cell function in obesity and diabetes. *Trends Mol. Med.* **8**, 442-447.

Chao, L., Marcus-Samuels, B., Mason, M. M., Moitra, J., Vinson, C., Arioglu, E., Gavrilova, O. and Reitman, M. L. (2000) Adipose tissue is required for the antidiabetic, but not for the hypolipidemic, effect of thiazolidinediones. *J. Clin. Invest.* **106**, 1221-1228.

Cobb, J. E., Blanchard, S. G., Boswell, E. G., Brown, K. K., Charifson, P. S., Cooper, J. P., Collins, J. L., Dezube, M., Henke, B. R., Hull-Ryde, E. A., Lake, D. H., Lenhard, J. M., Oliver, W., Jr., Oplinger, J., Pentti, M., Parks, D. J., Plunket, K. D. and Tong, W. Q. (1998) N-(2-benzoylphenyl)-l-tyrosine PPARγ agonists. 3. Structure-activity relationship and optimization of the N-aryl substituent. *J. Med. Chem.* **41**, 5055-5069.

Collins, J. L., Blanchard, S. G., Boswell, G. E., Charifson, P. S., Cobb, J. E., Henke, B. R., Hull-Ryde, E. A., Kazmierski, W. M., Lake, D. H., Leesnitzer, L. M., Lehmann, J., Lenhard, J. M., Orband-Miller, L. A., Gray-Nunez, Y., Parks, D. J., Plunkett, K. D. and Tong, W. Q. (1998) N-(2-benzoylphenyl)-l-tyrosine PPARγ agonists. 2. Struc-

ture-activity relationship and optimization of the phenyl alkyl ether moiety. *J. Med. Chem.* **41**, 5037-5054.
Elte, J. W. F. and Blickle, J. F. (2007) Thiazolidinediones for the treatment of type 2 diabetes. *Eur. J. Intern. Med.* **18**, 18-25.
Eom, S. H., Liu, S., Su, M., Noh, T. H., Hong, J., Kim, N. D., Chung, H. Y., Yang, M. H. and Jung, J. H. (2016) Synthesis of phthalimide derivatives as potential PPAR-γ ligands. *Mar. Drugs* **14**, 112.
Evans, R. M., Barish, G. D. and Wang, Y. X. (2004) PPARs and the complex journey to obesity. *Nat. Med.* **10**, 355-361.
Forman, B. M., Tontonoz, P., Chen, J., Brun, R. P., Spiegelman, B. M. and Evans, R. M. (1995) 15-Deoxy-Δ12, 14-prostaglandin J2 is a ligand for the adipocyte determination factor PPARγ. *Cell* **83**, 803-812.
Fujita, H., Kakei, M., Fujishima, H., Morii, T., Yamada, Y., Qi, Z. and Breyer, M. D. (2007) Effect of selective cyclooxygenase-2 (cox-2) inhibitor treatment on glucose-stimulated insulin secretion in c57bl/6 mice. *Biochem. Biophys. Res. Commun.* **363**, 37-43.
Henke, B. R., Blanchard, S. G., Brackeen, M. F., Brown, K. K., Cobb, J. E., Collins, J. L., Harrington, W. W., Jr., Hashim, M. A., Hull-Ryde, E. A., Kaldor, I., Kliewer, S. A., Lake, D. H., Leesnitzer, L. M., Lehmann, J. M., Lenhard, J. M., Orband-Miller, L. A., Miller, J. F., Mook, R. A., Jr., Noble, S. A., Oliver, W., Jr., Parks, D. J., Plunket, K. D., Szewczyk, J. R. and Willson, T. M. (1998) N-(2-benzoylphenyl)-L-tyrosine PPARγ agonists. 1. Discovery of a novel series of potent antihyperglycemic and antihyperlipidemic agents. *J. Med. Chem.* **41**, 5020-5036.
Higgins, L. S. and Mantzoros, C. S. (2008) The development of INT131 as a selective PPARγ modulator: approach to a safer insulin sensitizer. *PPAR Res.* **2008**, 936906.
Huang, S., Hu, H., Cai, Y.-H. and Hua, F. (2019) Effect of parecoxib in the treatment of postoperative cognitive dysfunction: a systematic review and meta-analysis. *Medicine* **98**, e13812.
Hu, Y., Stumpfe, D. and Bajorath, J. (2017) Recent advances in scaffold hopping. *J. Med. Chem.* **60**, 1238-1246.
Jiang, T., Shi, X., Yan, Z., Wang, X. and Gun, S. (2019) Isoimperatorin enhances 3T3-L1 preadipocyte differentiation by regulating PPARγ and C/EBPα through the Akt signaling pathway. *Exp. Ther. Med.* **18**, 2160-2166.
Khanna-Gupta, A., Abayasekara, N., Levine, M., Sun, H., Virgilio, M., Nia, N., Halene, S., Sportoletti, P., Jeong, J.-Y., Pandolfi, P. P. and Berliner, N. (2012) Up-regulation of translation eukaryotic initiation factor 4E in nucleophosmin 1 haploinsufficient cells results in changes in CCAAT enhancer-binding protein α activity: implications in myelodysplastic syndrome and acute myeloid leukemia. *J. Biol. Chem.* **287**, 32728-32737.
Krey, G., Braissant, O., L'Horset, F., Kalkhoven, E., Perroud, M., Parker, M. G. and Wahli, W. (1997) Fatty acids, eicosanoids, and hypolipidemic agents identified as ligands of peroxisome proliferator-activated receptors by coactivator-dependent receptor ligand assay. *Mol Endocrinol.* **11**, 779-791.
Kroker, A. J. and Bruning, J. B. (2015) Review of the structural and dynamic mechanisms of pparγ partial agonism. *PPAR Res.* **2015**, 816856.
Leonardini, A., Laviola, L., Perrini, S., Natalicchio, A. and Giorgino, F. (2009) Cross-talk between PPARgamma and insulin signaling and modulation of insulin sensitivity. *PPAR Res.* **2009**, 818945.
Lipinski, C. A., Lombardo, F., Dominy, B. W. and Feeney, P. J. (1997) Experimental and computational approaches to estimate solubility and permeability in drug discovery and development settings. *Adv. Drug Deliv. Rev.* **23**, 3-25.
Liu, C., Feng, T., Zhu, N., Liu, P., Han, X., Chen, M., Wang, X., Li, N., Li, Y., Xu, Y. and Si, S. (2015) Identification of a novel selective agonist of PPARγ with no promotion of adipogenesis and less inhibition of osteoblastogenesis. *Sci. Rep.* **5**, 9530.
Mangelsdorf, D. J., Thummel, C., Beato, M., Herrlich, P., Schütz, G., Umesono, K., Blumberg, B., Kastner, P., Mark, M., Chambon, P. and Evans, R. M. (1995) The nuclear receptor superfamily: the second decade. *Cell* **83**, 835-839.
Morris, G. M., Huey, R., Lindstrom, W., Sanner, M. F., Belew, R. K., Goodsell, D. S. and Olson, A. J. (2009) AutoDock4 and AutoDockTools4: automated docking with selective receptor flexibility. *J. Comput. Chem.* **30**, 2785-2791.
Motoshima, K., Ishikawa, M., Hashimoto, Y. and Sugita, K. (2011) Peroxisome proliferator-activated receptor agonists with phenethylphenylphthalimide skeleton derived from thalidomide-related liver X receptor antagonists: relationship between absolute configuration and subtype selectivity. *Bioorg. Med. Chem.* **19**, 3156-3172.
Nolte, R. T., Wisely, G. B., Westin, S., Cobb, J. E., Lambert, M. H., Kurokawa, R., Rosenfeld, M. G., Willson, T. M., Glass, C. K. and Milburn, M. V. (1998) Ligand binding and co-activator assembly of the peroxisome proliferator-activated receptor-γ. *Nature* **395**, 137-143.
Petersen, R. K., Christensen, K. B., Assimopoulou, A. N., Fretté, X., Papageorgiou, V. P., Kristiansen, K. and Kouskoumvekaki, I. (2011) Pharmacophore-driven identification of PPARγ agonists from natural sources. *J. Comput. Aided Mol. Des.* **25**, 107-116.
Pettersen, E. F., Goddard, T. D., Huang, C. C., Couch, G. S., Greenblatt, D. M., Meng, E. C. and Ferrin, T. E. (2004) UCSF Chimera—a visualization system for exploratory research and analysis. *J. Comput. Chem.* **25**, 1605-1612.
Sanner, M. F. (1999) Python: a programming language for software integration and development. *J. Mol. Graph. Model.* **17**, 57-61.
Semple, R. K., Chatterjee, V. K. K. and O'Rahilly, S. (2006) PPARγ and human metabolic disease. *J. Clin. Invest.* **116**, 581-589.
Smith, U. and Kahn, B. B. (2016) Adipose tissue regulates insulin sensitivity: role of adipogenesis, de novo lipogenesis and novel lipids. *J. Intern. Med.* **280**, 465-475.
Su, M., Cao, J., Huang, J., Liu, S., Im, D. S., Yoo, J.-W. and Jung, J. H. (2017) The *in vitro* and *in vivo* anti-inflammatory effects of a phthalimide PPAR-γ agonist. *Mar. Drugs* **15**, 7.
Trott, O. and Olson, A. J. (2010) AutoDock Vina: improving the speed and accuracy of docking with a new scoring function, efficient optimization, and multithreading. *J. Comput. Chem.* **31**, 455-461.
Waku, T., Shiraki, T., Oyama, T. and Morikawa, K. (2009) Atomic structure of mutant PPARγ LBD complexed with 15d-PGJ2: novel modulation mechanism of PPARγ/RXRα function by covalently bound ligands. *FEBS Lett.* **583**, 320-324.
Wang, L., Waltenberger, B., Pferschy-Wenzig, E.-M., Blunder, M., Liu, X., Malainer, C., Blazevic, T., Schwaiger, S., Rollinger, J. M., Heiss, E. H., Schuster, D., Kopp, B., Bauer, R., Stuppner, H., Dirsch, V. M. and Atanasov, A. G. (2014) Natural product agonists of peroxisome proliferator-activated receptor gamma (PPARγ): a review. *Biochem. Pharmacol.* **92**, 73-89.
Wang, Q., Imam, M. U., Yida, Z. and Wang, F. (2017) Peroxisome proliferator-activated receptor gamma (PPARγ) as a target for concurrent management of diabetes and obesity-related cancer. *Curr. Pharm. Des.* **23**, 3677-3688.
Wang, Y., Chen, Z., Li, J. and Shi, J. (2019) Parecoxib improves the cognitive function of POCD rats via attenuating COX-2. *Eur. Rev. Med. Pharmacol. Sci.* **23**, 4971-4979.
Willson, T. M., Lambert, M. H. and Kliewer, S. A. (2001) Peroxisome proliferator-activated receptor γ and metabolic disease. *Annu. Rev. Biochem.* **70**, 341-367.
Younce, C. W., Azfer, A. and Kolattukudy, P. E. (2009) MCP-1 (monocyte chemotactic protein-1)-induced protein, a recently identified zinc finger protein, induces adipogenesis in 3T3-L1 pre-adipocytes without peroxisome proliferator-activated receptor γ. *J. Biol. Chem.* **284**, 27620-27628.